Eur. Phys. J. D **8**, 193–198 (2000)

THE EUROPEAN PHYSICAL JOURNAL D

EDP Sciences

Use of a fast beam target for the determination and reduction of the cascade contribution to electron excitation cross-section measurements

J.B. Boffard, M.F. Gehrke, M.E. Lagus[a], L.W. Anderson, and C.C. Lin[b]

Department of Physics, University of Wisconsin, Madison, WI 53706, USA

Received 19 April 1999 and Received in final form 10 August 1999

Abstract. This paper describes a method for reducing the influence of cascades on the measurement of electron excitation cross sections using the optical method and a fast beam atomic target. By using a fast beam of target atoms one can reduce the influence of cascades on a measurement, and estimate the cascade contribution to the excitation signal.

PACS. 34.80.Dp Atomic excitation and ionization by electron impact

1 Introduction

In the optical method for measuring electron-impact excitation cross-sections, the photon flux out of a particular excited level is proportional to the apparent cross-section of the level. Each upper level, however, is populated both by direct electron-impact excitation from the initial state, and by cascades from atoms initially excited into higher lying levels that radiatively decay into the upper level of interest. Since direct excitation is the underlying fundamental process for populating all the various levels, determination of the direct cross-section requires the subtraction of the cascade contribution to the measured apparent cross-section. The difficulties of performing a full cascade subtraction remains one of the major problems of the optical method [1,2], since it requires measuring many additional transitions which are often in the infrared (IR) region of the spectrum where optical detection is difficult. While it is possible in some cases to measure most of the important cascade transitions [3], one must often resort to using theoretical estimates for some of the cascade contributions [1].

Time-resolved studies have provided one way to handle the problems cascades pose. For a pulsed electron beam, the cascade contribution to an excitation process can be deduced from the temporal dependence of the fluorescence. By fitting the observed time dependence to the sum of exponential terms corresponding to the lifetimes of the excited level in question and the levels that cascade into it, one can obtain the fractional contributions to the apparent excitation cross-sections from the cascading levels. This method, pioneered by Hughes and his coworkers, has been applied to various levels of He [4]. For example, the helium 3^3D level receives cascades from the n^3P and nF levels. The cascade transitions from the F levels are difficult to measure directly by photomultiplier tubes (PMT) since they lie in the infrared. The lifetimes of the 4^3P (154 ns), 4F (72 ns) and the 5F (138 ns) cascading levels, however, are much longer than the lifetime of the 3^3D level (14 ns). Thus, it has been possible to measure the nF cascade cross-sections by monitoring the time dependence of the easily visible $3^3\mathrm{D} \rightarrow 2^3\mathrm{P}$ (587.6 nm) transition at the termination of an electron beam pulse [4]. The 4F and 5F cascade cross-sections so determined are in reasonable agreement with subsequent direct measurements of the $n\mathrm{F} \rightarrow 3^3\mathrm{D}$ emissions by infrared Fourier transform spectroscopy [5]. It is also possible to use time-resolved techniques to virtually eliminate the cascade contribution to the detected signal [6]. In the first few nanoseconds of an electron beam pulse, the fluorescence from a given level will be almost solely the result of direct excitation, since any cascading levels will not yet have had time to decay into the level of interest.

In this paper we report on an approach to determining the cascades by means of a fast beam target. The fast beam target permits a form of time-resolved experiment to be performed akin to beam-foil spectroscopy where the thin foil is replaced by an electron beam. The time dependence of the cascading levels is mapped into an easily detected spatial dependence of the fluorescence down stream from the electron beam.

2 Apparatus

Near-resonant charge exchange between fast ions and an alkali vapor can be used to create metastable atoms of all the noble gases and hydrogen. A complete description of the apparatus we have used to measure electron-impact

[a] *Present address*: IBM Corp., Hopewell Junction, NY 12533, USA.

[b] e-mail: `cclin@facstaff.wisc.edu`

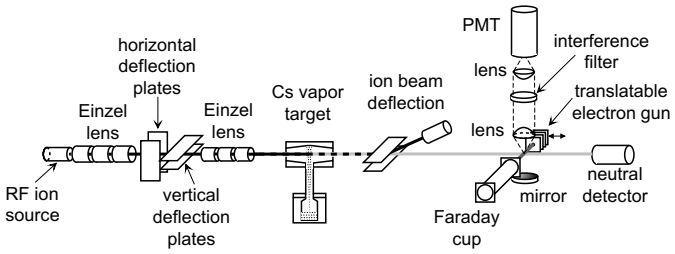

Fig. 1. Experimental apparatus.

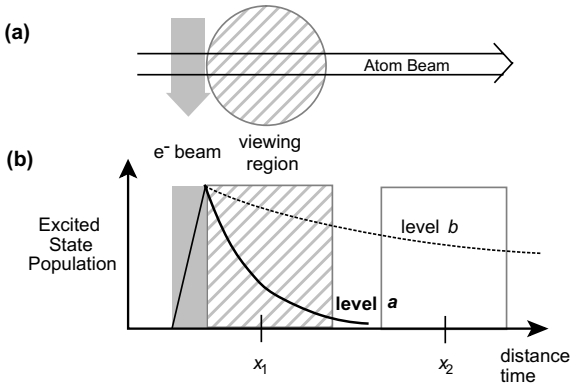

Fig. 2. (a) The atom beam first passes through the electron beam, and then the fluorescence from decaying atoms is gathered from a viewing region located some distance downstream. (b) The motion of atoms in the fast beam targets converts the spatial dimensions of the apparatus (the widths of the electron beam and viewing region) into temporal periods, while the temporal decay of excited levels are mapped into a spatial decay patterns.

excitation out of the metastable levels of helium [7] and argon [8] is given elsewhere [7,9]; in this paper we only discuss those details necessary for the cascade measurements.

A schematic diagram of our apparatus is shown in Figure 1. Helium or argon ions are extracted from an RF ion source and accelerated to an energy of 1.6 keV for helium and 2.1 keV for argon. The ion beam is partially converted into a neutral beam by passing the beam through a cesium vapor target. Metastable atoms are formed *via* near-resonant charge-transfer between the rare-gas atoms and the ground state of cesium. For helium, this process yields a neutral target beam in excess of 85% metastable atoms [10,11]; in the case of argon, roughly 40% of the neutral target is in metastable levels [11,12]. The ground state atoms in the fast beam make a negligible contribution to the excitation signal since the excitation cross-sections out of the ground level are much smaller than the corresponding metastable excitation cross-sections.

The remaining ions are removed from the fast beam by an electrostatic deflector, and the fast neutral beam is crossed at right angles by a variable energy electron beam. The fluorescence produced by electron excitation is detected at right angles to both the electron beam axis and the atomic beam axis with a narrow bandwidth interference filter and a GaAs PMT. The electron gun is mounted on a translation stage such that it can be moved ± 1 cm from the center of the optical detection axis in a direction parallel to the fast atomic beam. The fast atomic beam flux is measured with a neutral beam detector located in a separate beam dump chamber. Further information on data acquisition procedures, absolute calibration, and data reduction can be found in our earlier works [7,8].

3 Method and results

3.1 Qualitative illustration of method

To illustrate our general method consider the collision region as shown in Figure 2. Figure 2a is a schematic representation of the fast atom beam, electron beam, and the viewing region from which photons are collected. The distance between the point of electron excitation and fluorescence detection can be converted into a delay time since the incident fast atomic beam travels this length in a time equal to the distance divided by the atomic beam velocity. The velocity of a 1.6 keV He beam is 0.3 mm/ns, while the velocity of a 2.1 keV Ar atom is equal to 0.1 mm/ns. Indicated in Figure 2b is the normalized excited state population for two levels with different lifetimes as a function of the position along the atomic beam axis. Before the atoms in the fast beam reach the electron beam, the excited state populations are zero. As the atoms pass through the electron beam the number of atoms in the two excited states increases. Without cascades, there is no mechanism to produce excited state atoms after leaving the electron beam so the populations follow simple exponential decay functions. With the addition of cascades, the spatial decay functions contain terms involving both the lifetime of the particular level of interest and the lifetimes of all the levels that cascade into the excited state of interest. Thus the time dependence of an excited state population can be monitored by studying the fluorescence as a function of the position along the atomic beam axis.

Let us now consider the case where we observe the fluorescence from the decay of atoms in level-a, where atoms in level-a are populated both by direct excitation and also by cascades from the long-lived level-b. We further assume that the cross-section for excitation into both levels are equal, so that the populations in each level at the end of the very short electron beam "pulse" are equal. If the electron gun is positioned such that optical viewing region is at position x_1 (Fig. 2b) virtually all of the atoms created by direct excitation decay before leaving the viewing region. On the other hand, only a relatively small fraction of the atoms excited into level-b have decayed into level-a within the viewing region. Thus virtually all of the light collected from atoms decaying out of level-a will be from atoms created by direct excitation. If the electron gun is positioned such that the viewing region is located far downstream from the electron beam (position x_2 in Fig. 2b), the detected fluorescence is almost entirely due to atoms populated by cascades since the atoms excited directly into level-a have almost all decayed before reaching the viewing region.

The fast beam experiment thus lends itself to two modes of operation. First, by fixing the location of the

Table 1. Reduction in the cascade contribution to the measured apparent cross-section for excitation of the n^3L levels of helium from the 2^3S metastable level. Data at 10 eV.

for excitation into	Q^{casc}/Q^{app} from [13]	Q^{casc}/Q^{app} for 1.6 keV fast beam target
3^3S	8%	2%
3^3P	53%	10%
3^3D	6%	$< 1\%$
4^3D	11%	$< 1\%$

electron beam at the start of the viewing region, the effects of cascades on the measured signal are minimized. The cascade reduction is largest if the cascading levels have lifetimes much longer than the level of interest, but there is still a cascade reduction even if the cascading level has a lifetime equal to or less than the level of interest (although the magnitude of the cascade reduction is lower). This is due to the fact that a cascading level must always undergo two decays before it is detected. A second mode of operation is to study the fluorescence as a function of the separation between the electron beam and the optical viewing region. The shape of the resulting fluorescence curve enables one to estimate the size of the cascade cross-section. The cascade reduction method is illustrated in the following section using excitation of metastable helium, while the cascade estimation method is illustrated in Section 3.3 using excitation of metastable argon. All results were analyzed using the quantitative model outlined in the Appendix.

3.2 Cascade reduction

To illustrate the cascade reduction of a fast beam target, let us briefly consider electron excitation out of the He(2^3S) metastable level into the n^3L levels where the cascade contributions to the apparent cross-sections have been measured by Piech *et al.* [13] in a non-time-resolved experiment for excitation up to the $n = 8$ levels. Table 1 indicates the percentage of the measured apparent cross-section that is due to cascades for an incident electron energy of 10 eV. If the known cross-sections of reference [13] are combined with lifetimes and branching fractions for the cascading levels, we can model the contribution of the cascading levels for a fast beam target when the signal is acquired with the viewing region immediately after the electron gun. As seen in the second column of Table 1, the cascade contribution is greatly diminished [7]. For the levels studied, there is at least a factor of four reduction in cascades, with a much greater reduction for the n^3D levels. Thus it is possible to obtain almost cascade-free excitation cross-sections from a fast beam target.

3.3 Cascade measurement

We demonstrate the cascade measurement capability of the fast beam target by considering excitation out of the $3p^5 4s J = 2$ metastable level of argon ($1s_5$ in Paschen's notation) into levels of the $3p^5 4p$ configuration ($2p_n$ in Paschen's notation). Fluorescence out of the ten levels of the $3p^5 4p$ configuration lie in the 700–900 nm wavelength range accessible by PMTs. The largest contribution to the cascades for these levels is from the levels of the $3p^5 5s$ and $3p^5 3d$ configurations. The transitions from these levels lie in the infrared making their measurement difficult. Further, there are no existing theoretical or experimental values for these levels upon which to estimate the cascade contribution to the $3p^5 4p$ apparent cross-sections.

The 0.1 mm/ns velocity of the Ar* fast atomic beam converts the ~ 2 mm wide electron beam into a 25 ns long pulse. This is comparable to the radiative lifetime of the $3p^5 4p$ levels which have lifetimes between 22–39 ns, and consequently the excited state atom density in the atomic beam does not reach a steady-state value. First consider excitation into the $2p_9$ ($J = 3$) level which has a lifetime of 30 ns. The primary cascades into this level are from the $J = 2, 3$ and 4 levels of the $3p^5 5s$ and $3p^5 3d$ configurations with lifetimes ranging from 45 to 175 ns. The curves in Figure 2b correspond to case where we associate level-a with the $2p_9$ level and level-b with the $3d'_1$ level of the $3p^5 3d$ configuration which has a lifetime of 175 ns. With the viewing region immediately after the electron beam, 90% of the $2p_9$ atoms created by direct excitation will decay before exiting the viewing region; but only 30% of the atoms in the $3d'_1$ cascade level will have decayed into the $2p_9$ level within the viewing region. To contribute to the observed $2p_9 \rightarrow 1s_5$ fluorescence (811.5 nm) these atoms must further decay out of the $2p_9$ within the viewing region. As a result, only about 17% of the atoms excited into the $3d'_1$ level will contribute to the measured fluorescence signal. This corresponds to over a factor of five reduction in the cascade contribution from this level. The other cascading levels all have shorter lifetimes so the reduction will be less, although even a level with a lifetime of 45 ns still has a cascade reduction factor of approximately two.

When the viewing region is moved farther downstream from the electron excitation region the situation gradually changes. Fewer of the $2p_9$ atoms created by direct excitation survive to decay within the viewing region. Nevertheless, atoms continue to populate the $2p_9$ level from the decay of long lived cascading levels. At large separations atoms populated by these cascades result in more fluorescence signal than those due to direct excitation. The magnitude of the increased signal is an indication of the size of the otherwise unmeasured cascade cross-sections.

As a further example, let us consider the $3p^5 4p$ ($J = 2$) $2p_6$ level of argon with a lifetime of 29 ns. The $2p_6$ level receives most of its cascades from the same cascading levels as the $2p_9$ level, with the addition of the $J = 1$ levels of the $3p^5 5s$ and $3p^5 3d$ configurations. These additional $J = 1$ levels also have resonance transitions to the ground state, and have lifetimes much less than 20 ns which would make it difficult to see the changes in the shape of the $2p_6$ fluorescence curve if there were a substantial cascade contribution from these levels. However, the branching fraction to the ground state for these short-lived levels is much larger

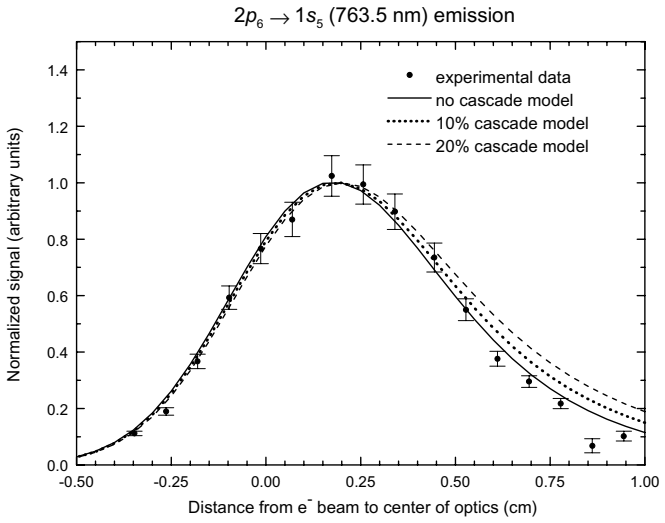

Fig. 3. Cascade analysis of argon $2p_6$ level for an electron energy of 50 eV. Note that the electron beam is centered under the optics for $x = 0$. The peak of the fluorescence signal occurs when the electron beam is moved upstream by its width (0.22 cm).

than the branching fraction to the $2p_6$ level. Hence, very few of the atoms excited to these levels decay to the $2p_6$ level and thus contribute to the $2p_6$ fluorescence. Instead, most of the $2p_6$ cascades are from levels with lifetimes in the range of 45 ns and up. To estimate the cascade contribution we assume the worst case scenario of a cascading level with a lifetime of 45 ns and calculate the $2p_6 \rightarrow 1s_5$ (763.5 nm) emission signal as a function of the distance between the viewing region and the electron beam. The modeled signal in which the $2p_6$ level is populated both by direct electron-impact excitation and by varying amounts of cascades is shown in Figure 3. Details of this calculation are described in the Appendix. A least squares fit to the experimental data indicates the cascade to direct cross-section ratio (r_{jk}) is less than 0.04 ± 0.04. A fit to the data for the $2p_9$ level [14] indicates a cascade to direct cross-section ratio of 0.09 ± 0.04.

A number of factors influence the ultimate uncertainties in the measured cascade cross-sections. The largest sources of uncertainty (including the measurements of the metastable beam flux, the intensity and polarization of the radiation) are related to the absolute calibration of the cross-sections. They have the effect of altering the apparent excitation cross-sections by a multiplicative factor but do not change the percentage cascade in the apparent cross-sections. Uncertainties of this kind have been discussed in our earlier papers [7–9] and the interested reader is referred to those publications for details. In this paper we are more concerned with the error sources that would affect the ratio of cascades to the apparent cross-sections. Such error sources are limited to the measurement of the electron beam and optical profiles, and any changes in the overlap of the electron beam and atomic beam as the electron-gun is transversed along the atomic beam axis. The profile functions are checked by filling the collision chamber with a static gas target and comparing the signal with a modeled low-velocity beam. To minimize the effect of any misalignment of the electron-gun displacement axis with the fast atom beam axis, a wide atomic beam is used.

As described in Section 3.1, when the viewing region is located close to the electron beam, the cascade contribution is further diminished. Hence using a fast beam target we are able to demonstrate that the cascade cross-sections into the $2p_6$ and $2p_9$ levels are small, and we are further able to minimize the contribution of this small cascade contribution. In this case the apparent cross-sections measured with the viewing region immediately after the electron beam are good approximations to the direct excitation cross-sections without any cascade corrections since cascades make no more than a 5% contribution to the apparent cross-section. Since the objective of our measurements is the direct cross-section, the fact that we can demonstrate that we have only a negligible amount of cascade in our raw signal is most appealing.

4 Discussion

It is useful to place the present technique in context of: first, other means of cascade measurement and reduction; and second, other uses of a fast beam target. Methods of obtaining cascade measurements, besides direct observation, include the time-resolved techniques mentioned in Section 1, and photon coincidence measurements [15]. The later technique involves measuring a photon in coincidence with an inelastically scattered electron of the proper energy. As such, it more closely related to electron-energy loss measurements than the techniques based on optical method that we are concerned with.

The most obvious means of determining the cascade contribution is the monitoring of the fluorescence from the cascading transitions. Direct optical measurement of cascades is desirable since it provides information on the size and energy dependence of additional higher lying levels. This bonus information comes at the cost of additional measurements in possibly difficult regions of the spectrum. In the case of the argon levels considered in Section 3.3 the wavelengths of the main cascades lie in the near IR: 0.9 to 1.7 μm for the $3p^5 5s \rightarrow 3p^5 4p$ transitions, and 1.1 to 2.4 μm for the $3p^5 3d \rightarrow 3p^5 4p$ transitions. The IR detectors needed in this wavelength regime have much lower sensitivities than the PMT we used to measure the transitions from the decay of the $3p^5 4p$ levels. The minimum detectable excitation signal we can extract from the background with our photon-counting based detection system is in the range of 10^{-18} to 10^{-19} W (at the PMT), while the typical signal sizes used in our cascade analysis work were about two orders of magnitude above this. The IR detectors used to directly measure the cascade cross-sections into the $2p$ levels for ground state electron-impact excitation [3] had minimum detectable powers of about 10^{-16} W for $\lambda \leq 1.6$ μm (InGaAs detector), and around 10^{-15} W for $\lambda > 1.6$ μm (InSb detector). For the typical parameters of the fast beam target (target density, electron current...), this would translate into a minimum detectable cascade

cross-section of about 10^{-15} cm^2. This provides no real constraint on the cascade contribution for the levels considered here since this minimum is larger than the *sum* of the direct *and* cascade cross-sections of the $2p_6$ level (5×10^{-16} cm^2 at 50 eV) and $2p_9$ level (12×10^{-16} cm^2 at 50 eV) [8]. Using a hollow cathode discharge as a source of metastable atoms [16] would result in approximately two orders gain in target density which may raise the signal rate of the strongest cascade levels above the measurable limit. However, this source has other limitations [8], and the sum of all the cascade cross-sections will still have larger uncertainties than the limit established by the fast beam method.

Another way to determine the cascade contribution to the apparent excitation cross-sections is to measure the time dependence of the radiation emitted by excited atoms after the cessation of a pulsed electron beam, as described in Section 1. Standard time-resolved experiments have a very low duty factor (less than 0.1%) [6] since the timing between electron beam pulses must be on the order of the longest-lived excited state present in the system. In contrast, the techniques of beam-foil spectroscopy allows similar time resolved measurements to be made with a CW source. By using a fast atomic beam, the temporal dependence of the radiation is mapped into a spatial dependence of the fluorescence signal, not by pulsing the electron beam. The signal at a given separation of the electron beam and optical detection region is time independent. Even with a double modulation of both the electron beam and neutral beam we can still achieve a 25% duty factor.

Fast beam targets have been used for many years in the field of beam-foil spectroscopy. The spatial distribution of excitation in a fast beam emerging from a thin-foil provides an effective means of measuring the lifetimes of cascading levels. However, the amounts of cascades obtained in a beam-foil experiment do not correspond to the apparent excitation cross-sections in the context of single electron-atom collision processes. Atomic collision cross-sections can be measured by replacing the foil target with either a gas jet [17] or atomic beam [18]. For example, Aumayr *et al.* [18] have studied electron capture collisions between a fast H^+ beam and a Li atomic beam. The cross-sections for capture into the three different H ($n = 3$) levels were deduced from how the lifetimes of the levels affected the spatial profile of the emissions downstream from the Li target. In contrast to these uses of a fast beam, most previous electron-impact experiments using a fast beam have not fully exploited the time-resolved aspects of such a target. The previous electron-impact works with fast atom beams formed *via* charge transfer have mainly studied ionization [19,20], and thus were unconcerned with the temporal pattern of fluorescence. There has been, however, work done on electron-impact excitation of fast ions which have included the time dependence of the emission signal [21,22]. As a particular example, Rogers *et al.* [22] have measured the excitation of $Li^+(2^3S)$ into the 2^3P level. Due to the motion of the fast ions out of the viewing region, the authors had to correct for the fact that about 65% of the excited ions decayed beyond their detection region. No experiments on moving the electron beam away from the viewing axis were reported. Nevertheless, the primary cascades into the 2^3P level had lifetimes much shorter than the 2^3P level, so the reduction to the cascade contribution was minimal.

The significant disadvantage in working with a fast beam target is the very small target density. The fast beam experiment typically operates with 1 particle μA in a 7 mm diameter beam, which corresponds to a target density of only 10^6 atoms/cm^3. This is about seven orders of magnitude smaller than the target densities employed in typical gas target electron-excitation experiments ($\sim$ 1 mtorr). One reason why we are able to overcome this drastically reduced number density is that we are studying excitation out of the metastable levels which have excitation cross-sections two to three orders of magnitude larger than cross-sections out of the ground level.

With sufficient time resolution it is possible to fit multiple exponential decay curves to the data and obtain values for the contribution from each of the cascading levels. Our time resolution is relatively poor (tens of nanoseconds), which prevent us from doing a more elaborate analysis [23]. The time resolution of the experiment is determined by the physical sizes of the electron beam and optical viewing region as well as the atomic beam velocity. Thus, one can dramatically improve the time resolution by either narrowing the size of the viewing region, or using a higher velocity atomic beam. Both of these measures would also lead to commensurate reductions in our already low signal rate. Since our objective is the measurement of direct excitation cross-sections, and we have demonstrated that by using the fast-beam target the cascade component of the apparent cross-section is reduced to less than the statistical uncertainty in the measured cross-sections for all the cases discussed in this paper, it is not necessary for our purposes to determine the contributions from each cascading level separately.

5 Conclusions

The present technique combines the key feature of beam-foil spectroscopy in mapping the time-dependence of atomic emission into a spatial dependence with the method of Hughes *et al.* in using the time resolution of the atomic emission to determine the cascade contribution to apparent excitation cross-sections. By studying the variation in the fluorescence intensity as a function of the distance between the electron excitation region and the optical detection region, it is possible to estimate (or at least place limits on) the size of the cascade cross-section. It is also possible to reduce the cascade contribution to the detected signal by positioning the optical viewing region at the end of the effective electron pulse. Thus, the uncertainties introduced into direct cross-section measurements by cascades can be significantly reduced. Because of the inherent low density of the fast beam atomic target, this method has only been applied to excitation out of the metastable atoms for which the excitation cross-sections are large. However, it should be possible to apply

this method to excitation of ions and ground-state atoms for excitation processes with large cross-sections.

This work was supported by the U.S. National Science Foundation.

Appendix: Quantitative model

A more quantitative cascade analysis requires the use of the measured profiles of the electron beam and the optical detection system. For the purposes of this analysis, we include only one level k that cascades into the level of interest j. The number of atoms in each excited level (N_j and N_k) as a function of the position x along the neutral beam axis can be found from the solution of the pair of coupled differential equations:

$$\frac{\mathrm{d}N_j(x)}{\mathrm{d}x} = Cj_\mathrm{e}(x) - \frac{N_j(x)}{v_\mathrm{f}\tau_j} + \Gamma_{kj}\frac{N_k(x)}{v_\mathrm{f}\tau_k}, \tag{A.1}$$

$$\frac{\mathrm{d}N_k(x)}{\mathrm{d}x} = r_{kj}Cj_\mathrm{e}(x) - \frac{N_k(x)}{v_\mathrm{f}\tau_k}, \tag{A.2}$$

where $j_\mathrm{e}(x)$ is the profile of the electron beam, v_f is the velocity of atoms in the fast beam, τ_i is the lifetime of the level-i, Γ_{kj} is the branching fraction of level k to level j, r_{jk} is the ratio of the direct cross-sections for level k and level j, and C is a constant that is proportional to the target density and cross-section for excitation into level j. The measured electron beam profile is well approximated by a Gaussian profile with a 2.2 mm FWHM. Our coordinate system is chosen such that the electron beam is centered at $x = 0$, so the excited level populations before the electron beam (large negative x values) is zero. The relative probability of detecting a photon emitted at a distance from the center of the optical system is given by the optical profile $\Phi(\Delta)$. The measured fluorescence signal is proportional to the number of decays at each point along the x-axis multiplied by the relative optical detection efficiency Φ at that point, integrated over the entire viewing region. If the center of the electron beam is displaced a distance d from the center of the optical detection region the signal is equal to

$$\begin{aligned} S(d) &= \int \Gamma_{jl}\frac{N_j(x)}{v_\mathrm{f}\tau_j}\Phi(x-d)\mathrm{d}x \\ &= S_0\int N_j(x)\Phi(x-d)\mathrm{d}x, \end{aligned} \tag{A.3}$$

where S_0 is a normalization constant. The relative efficiency of the optical detection system $\Phi(\Delta)$ has also been found to have a Gaussian profile with a 4.8 mm FWHM. Using this model we numerically calculate how the fluorescence signal for a particular level is expected to vary as a function of the distance between the center of electron beam and the center of the optical viewing region. Due to the arbitrary normalization constant S_0 in equation (A.3), we only compare the shapes of the experimental and modeled data; however, this comparison is sufficient to extract the ratio of the direct to cascade cross-sections r_{jk}.

References

1. D.W.O. Heddle, J.W. Gallagher, Rev. Mod. Phys. **61**, 221 (1989).
2. A.R. Filippelli, C.C. Lin, L.W. Anderson, J.W. McConkey, Adv. At. Mol. Opt. Phys. **33**, 1 (1994).
3. See for example J.E. Chilton, J.B. Boffard, R.S. Schappe, C.C. Lin, Phys. Rev. A **57**, 267 (1998).
4. See, for example, W.R. Pendeton Jr, R.H. Hughes, Phys. Rev. **138**, A683 (1965); R.J. Anderson, R.H. Hughes, T.G. Norton, Phys. Rev. **181**, 198 (1969); R.B. Kay, C.G. Simpson, J. Phys. B **21**, 625 (1988).
5. J.E. Chilton, C.C. Lin, Phys. Rev. A **58**, 4572 (1998).
6. I.P. Bogdanova, S.V. Yurgenson, Opt. Spektrosk. **61**, 20 (1986) [Opt. Spectrosc. **61**, 12 (1986)]; I.P. Bogdanova, S.V. Yurgenson, Opt. Spektrosk. **61**, 241 (1986) [Opt. Spectrosc. **61**, 156 (1986)].
7. M.E. Lagus, J.B. Boffard, L.W. Anderson, C.C. Lin, Phys. Rev. A **53**, 1505 (1996).
8. J.B. Boffard, G.A. Piech, M.F. Gehrke, L.W. Anderson, C.C. Lin, Phys. Rev. A **59**, 2749 (1999).
9. J.B. Boffard, M.E. Lagus, L.W. Anderson, C.C. Lin, Rev. Sci. Instrum. **67**, 2738 (1996).
10. C. Reynaud, J. Pommier, Vu Ngoc Tuan, M. Barat, Phys. Rev. Lett. **43**, 579 (1979).
11. R.H. Neynaber, G.D. Magnuson, J. Chem. Phys. **65**, 5239 (1976).
12. M.J. Coggiola, T.D. Gaily, K.T. Gillen, J.R. Peterson, J. Chem. Phys. **70**, 2576 (1979).
13. G.A. Piech, J.E. Chilton, L.W. Anderson, C.C. Lin, J. Phys. B **31**, 859 (1998).
14. J.B. Boffard, G.A. Piech, M.F. Gehrke, M.E. Lagus, L.W. Anderson, C.C. Lin, J. Phys. B **29**, L795 (1996).
15. See, for example, R.E. Imhof, F.H. Read, Nucl. Instrum. Meth. **90**, 109 (1970).
16. R.B. Lockwood, L.W. Anderson, C.C. Lin, Z. Phys. D **24**, 155 (1992).
17. N. Andersen, K. Jensen, C.S. Newton, K. Pedersen, E. Veje, Nucl. Instrum. Meth. **90**, 299 (1970).
18. F. Aumayr, M. Fehringer, H. Winter, J. Phys. B **17**, 4185 (1984).
19. For ionization of ground state atoms, see for example R.C. Wetzel, F.A. Baiocchi, T.R. Hayes, R.S. Freund, Phys. Rev. A **35**, 559 (1987).
20. For ionization of metastable atoms, see for example A.J. Dixon, A. von Engel, M.F.A. Harrison, Proc. R. Soc. Lond. A **343**, 333 (1975); or M. Johnston, K. Fujii, J. Nickel, S. Trajmar, J. Phys. B **29**, 531 (1996).
21. See for example P. Taylor, G.H. Dunn, Phys. Rev. A. **8**, 2304 (1973).
22. W.T. Rogers, J.Ø. Olsen, G.H. Dunn, Phys. Rev. A **18**, 1353 (1978).
23. See for example, L.J. Curtis, R.M. Schectman, J.L. Kohl, D.A. Chojnacki, D.R. Scoffstall, Nucl. Instrum. Meth. **90**, 207 (1970).